DEM-CFD Modeling of Particle Systems with Long-Range Electrostatic Interactions

Chunlei Pei and Chuan-Yu Wu
Dept. of Chemical and Process Engineering, University of Surrey, Guildford GU2 7XH, U.K.

David England and Stephen Byard
Sanofi-Aventis, U.K.

Harald Berchtold
Sanofi-Aventis Deutschland GmbH, Frankfurt, Germany

Michael Adams
School of Chemical Engineering, University of Birmingham, Birmingham B15 2TT, U.K.

DOI 10.1002/aic.14768
Published online March 26, 2015 in Wiley Online Library (wileyonlinelibrary.com)

To investigate dynamic behaviors of monocharged particle systems, a direct truncation (DT) method and a hybrid particle-cell (HPC) method are implemented into the discrete element method coupled with computational fluid dynamics (DEM-CFD) with defined cutoff distances. The DT method only considers electrostatic interactions between particles within the cutoff distance while the HPC method computes electrostatic interactions in the entire computational domain. The deposition process of monocharged particles in a container in air was simulated using the developed DEM-CFD. It was found that using the DT method, the macrostructure, evolution of granular temperature, and radial distribution function of the particle system were sensitive to the specified cutoff distance. In contrast, using the HPC method, these results were independent of the specified cutoff distance, as expected. This implies that, although electrostatic interactions between particles with large separation distances are weak, they should be considered in DEM-CFD for accurate modeling of charged particle systems. © 2015 American Institute of Chemical Engineers *AIChE J*, 61: 1792–1803, 2015
Keywords: electrostatics, discrete element method, long-range interaction, charged particle, hybrid particle-cell model, DEM-CFD

Introduction

Particles with contact potential difference can acquire electrostatic charges during contacts/collisions in various powder handling processes.[1–3] The attractive and repulsive electrostatic interactions can lead to aggregation and segregation of the particles[4,5] and unexpected particle dispersion.[6] This can significantly affect the efficiency of the corresponding powder handling process and the quality of the final products. Therefore, understanding the dynamics of electrostatically charged particles is very important in powder handling and processing.

The electrostatic interactions among particles can be determined explicitly or implicitly.[7–9] The explicit method generally determines the electrostatic force directly based on the distance between objects and the charge of the objects while the implicit method first calculates the electric potential for the given charge density distribution in the electric field, then the electric strength and the subsequent electrostatic interactions are determined.

Using the explicit method, the electrostatic interactions are generally determined based on the Coulomb's law in which the electrostatic force is a function of the charge of particles and the distance between particles. If the distance between particles is sufficiently large, the electrostatic force can be adequately and accurately determined from the total charge of the particles that is calculated by summing up elementary point charges on each particle.[7,9] If the separation distance between the charged objects is relatively small compared to the size of the charged objects, the charged object cannot be considered as a point charge because of the redistribution and polarization of the elementary charge on the surface of the object. The explicit method should hence be applied to the elementary charge on the surface of the object rather than the object. In reality, charge redistribution and image effects induced by polarization depend on material electrical properties, such as resistivity and permittivity. For insulating materials (dielectrics) with a high resistivity (e.g., $>10^{13}$ Ωm), the charge redistribution is a relative slow process, compared to the rapid particle collisions and separation during the powder

Current address of David England: Private Consultant.
Current address of Stephen Byard: Covance Laboratories, Alnwick, Northumberland NE66 2JH, U.K.

Correspondence concerning this article should be addressed to C. Y. Wu at C.Y.Wu@Surrey.ac.uk.

handling process.[10] In addition, the electrostatic analysis shows that the image interactions between dielectric materials can be very complicated and influenced by the charge, separation distance, and dielectric constants.[9] For insulating materials with a low polarizability (e.g., dielectric constant is close to 1), the effect of polarization is negligible. For instance, the electrostatic force between two spheres with the above material is very similar to that between two point charges at a relatively close separation distance (<10% of the sphere diameter). Conversely, Korevaar et al.[11] analyzed the influence of the attractive image interactions between particles and pipe walls made from grounded and conductive materials on the particle distribution during pneumatic conveying. It was found that the image force can attract particles to move toward the pipe walls and eventually retain particles at the wall, when the charge of the particles is high enough. Therefore, when the explicit method is used, the electrostatic interactions between objects should be considered according to the material properties and the process conditions.

However, the efficiency of the explicit method is limited by the number of particles (point charges). Theoretically, due to the long-range nature, electrostatic interactions between all particles in a system should be considered, which is very compute-intensive with a computational time up to $O(N^2)$ for a system of N particles. As the electrostatic force generally decreases with increasing separation distance, r, according to the power law function, r^{-2}, and it becomes very weak when the separation distance is large, a direct truncation (DT) method was then introduced to improve the computational efficiency.[8,12] In the DT method, a cutoff distance is specified and only electrostatic interactions between particles with a separation distance less than the cutoff value were considered. Electrostatic interactions between particles with a larger separation distance than the cutoff value were ignored. The computation efficiency depends on the cutoff distance; the speed is inversely related to the cutoff distance. The DT method is a simple approach that can significantly reduce the computational time. However, it may cause some artificial effects or introduce computational errors due to the exclusion of long-range electrostatic interactions.

The implicit method can be used to consider the entire particle system and the associated electric field. The potential distribution of an electric field is first calculated from the charge distribution by solving Poisson's equation that is derived from Gauss's law and energy conservation.[8] The electric potential distribution is then differentiated to obtain the electric field strength. The electrostatic forces are obtained from the product of the electrostatic charge and the electric field strength. The indirect method with an electric potential is commonly used in molecular dynamics (MD), plasma and astrophysics simulations, and for the applications in which the electric field and the charge distribution are of primary concern.[8]

The particle-mesh (PM) method[13] involves discretization of the electric field into a mesh with the charge on the particles mapped onto the nodes of the mesh in order to obtain the charge distribution. However, the calculation of the interactions between particles depends on the mesh density and the distribution of the particle. Consequently, the interactions between such neighboring particles cannot be determined accurately due to the extrapolation of charge distribution onto each mesh. To obtain a more accurate calculation, on the basis of the PM method, the particle–particle and particle-mesh (PP-PM) method[12,14,15] was developed. The electrostatic interaction between particles within the cutoff distance is calculated directly while the PM method is employed for particles located outside of the cutoff distance. In terms of the computational complexity, under periodic boundary conditions, the PP-PM method is superior to the Ewald method,[8] in which the short-range component is summed in real space and the long-range component is summed in Fourier space for MD and plasma simulations. To reduce the computational complexity in calculating the charge and potential distribution, some advanced methods such as the multipole expansion method can also be used.[16,17]

The discrete element method (DEM) has been widely used to analyze the dynamic behavior of particle systems.[18–21] It is a versatile method in which various interactions between particles including electrostatic forces can be modeled.[21] Recently, DEM has been applied to model charged particle systems.[5,16,22] Hogue et al.[22] modeled the flow of triboelectrically charged particles flowing down an inclined plane using DEM with unscreened and screened Coulomb force models. The former involved treating the charged particles as point charges while the latter introduced an additional term to consider the polarization effects of particles close to the reference particle. A screening radius was also applied to define a spherical space for calculating the charge concentration and determining the induced polarization effects. It was shown that, with the unscreened force model, particles spread to a larger angle on the inclined plane compared to that determined using the screened force model. However, the way in which the screening radius affects the spreading angle was not examined. Pei et al.[5] developed a coupled DEM with computational fluid dynamics (DEM-CFD) such that the electrostatic interactions were modeled using the DT method. They simulated the deposition of bicharged particles in a container with a cutoff distance of 10 particle radii. Due to the electrostatic forces between particles, the formation and breakage of agglomerates were observed in various deposition stages. Liu et al.[16] modeled the capture of particles onto a macroscopic electrode in an induced electric field, in which the dynamics of particles was analyzed using DEM; the electric field induced by particles near surfaces within a distance of 1.2 particle radii was computed with a boundary element method (BEM) and a hybrid BEM/image method. The electric field induced by distant particle charges was considered using an adaptive multipole expansion method. The numerical simulations confirmed the formation of "chain-like" aggregates on the macroscopic electrode. However, because of the computational complexity of BEM in calculating the charge distribution on the surface of spheres, the computational time will increase significantly if more particles are involved. In the previous DEM studies for charged particles, the DT method was generally used because of its computational efficiency. However, it is unclear whether artifacts and computational errors will be introduced as a result of neglecting long-range weak electrostatic forces.

Hence, the objective of this study is to explore if the DT method is sufficiently accurate for DEM modeling of charged particle systems, for which the DT method is implemented in our in-house DEM-CFD code. In addition, a hybrid particle-cell (HPC) method that considers the electrostatic interactions between all particles using a simplified explicit approach is also introduced and implemented into the DEM-CFD. In this article, both DT and HPC methods used in DEM are introduced in the next section. Using the

developed DEM-CFD with the DT and HPC models, deposition of monocharged particles in a container is simulated. In addition, deposition of neutral particles (without charge) is also modeled for reference. The structure of the deposited granular bed, the radial distribution function (RDF), and the granular temperature (GT) and their dependence on the cutoff distance of both methods are examined and discussed to evaluate the robustness of these methods for modeling charged particle systems. The computational time of both methods and the sensitivity of the HPC method to the cell size are also discussed.

Modeling Electrostatic Interaction Using DT and HPC Methods

The DEM-CFD method is developed to simulate the dynamics of particles during powder handling processes. The motion of particles in DEM is governed by Newton's second law under gravity, contact forces, particle-gas interactions, and electrostatic forces in each time step. The contact forces are determined using classical contact mechanics. For elastic particles considered in this study, the normal contact is modeled using Hertz theory[23] while the tangential interaction using the theory of Mindlin and Deresiewicz.[24] The compressible gas flow is governed by continuity and momentum equations and analyzed using an adapted SIMPLE scheme in CFD. The interactions between particles and air are simulated with the two-way coupling method. The details of this DEM-CFD method can be found in Kafui et al.[18,20]

To calculate the electrostatic interactions, both the DT and HPC methods are considered and implemented into the in-house DEM-CFD code. The electrostatic interactions are of great complexity due to the charge redistribution and polarization as discussed in Introduction section. To simplify the incorporation of electrostatic interaction into the DEM-CFD and examine DT and HPC methods in principle, it is assumed that (1) electrostatic charge on each particle is treated as a concentrated point charge at the center of the particle; (2) the induced electrostatic forces are governed by the Coulomb law; (3) image and polarization effects between interacting pair of particles are ignored; and (4) the physical boundaries (walls and surfaces) are always neutral and do not have electrostatic interactions with particles. In other words, the particles and containers in this study are assumed to be high insulating materials with low polarizability.

For both DT and HPC methods, a cell list is used to group and detect charged particles and their long-range electrostatic interactions in the computational domain, as illustrated in Figure 1. The domain is first divided into cells with a size greater than the diameter of the particle. All particles are then sorted into their corresponding cells based on the relative positions of the particles to the cells. As a result, each cell has its own particle list. A cutoff distance, R_c, is then introduced to define the maximum range of the electrostatic interactions. The total electrostatic force acting on particle i, $\mathbf{F}_i^e$ is determined as

$$\mathbf{F}_i^e = \sum_{j=1}^{n} \mathbf{F}_{ij}^e \tag{1}$$

where $\mathbf{F}_{ij}^e$ is the electrostatic force between particles i and j; Position A (PA): n is the number of particles

In the DT method, $\mathbf{F}_{ij}^e$ is given as

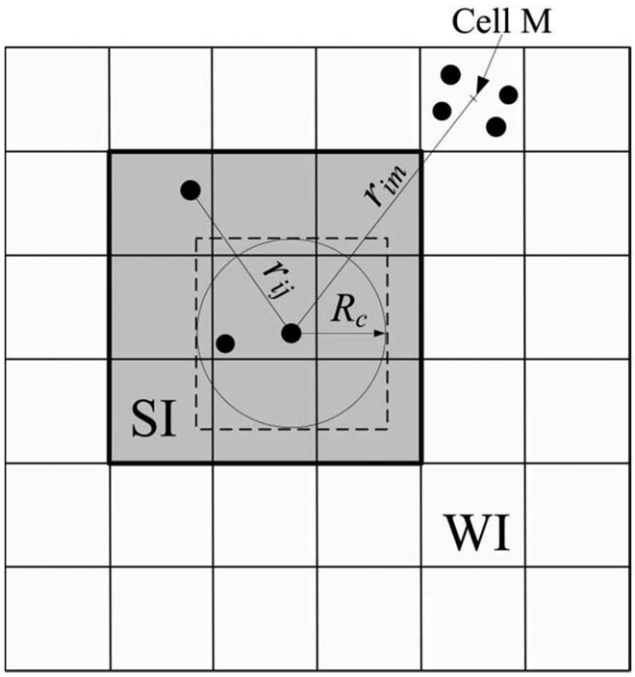

Figure 1. A 2-D illustration of the cell list method.

$$\mathbf{F}_{ij}^e = \frac{q_i q_j}{4\pi\varepsilon_0 r_{ij}^2}\mathbf{u}_{ij} \quad r_{ij} \le R_c \tag{2a}$$

$$\mathbf{F}_{ij}^e = 0 \quad r_{ij} > R_c \tag{2b}$$

where q_i and q_j are the net charge on the particles i and j; r_{ij} is the distance between the particles i and j; $\mathbf{u}_{ij}$ is the unit vector from particle j to particle i; and ε_0 is the permittivity of a vacuum (8.854×10^{-12} F/m). Equations 1 and 2 indicate that, in the DT method, only the electrostatic force between particles located within the cutoff distance is considered while electrostatic interactions between particles with a separation distance greater than the cutoff distance are ignored. This is similar to some published DEM models involving electrostatic interactions.[5,22]

In the HPC method, electrostatic interactions between all particles are considered in the following manner: for particle i, its electrostatic domain is divided into two regions using the specified cutoff distance R_c: a strong interaction (SI) region and a weak interaction (WI) region. The SI region is defined by the area of the mesh cells that envelops the circumscribed square/cube (the shaded area in Figure 1) of the cutoff circle/sphere while the cells outside the SI region constitute the WI region. The electrostatic force between particle i and any particle j located in the SI region is calculated directly using Eq. 2a. To determine the electrostatic interaction between particle i and those located in the WI region, the total net charge in each cell in the WI region is first calculated using

$$Q_M = \sum_{k=1}^{n_M} q_k \tag{3}$$

where n_M is the total number of particles in the cell M, Q_M, and q_k are the total charge of particles in the cell M and the charge of particle k, respectively. The electrostatic force between particle i and those in the cell M, $\mathbf{F}_{iM}$, is then approximated as

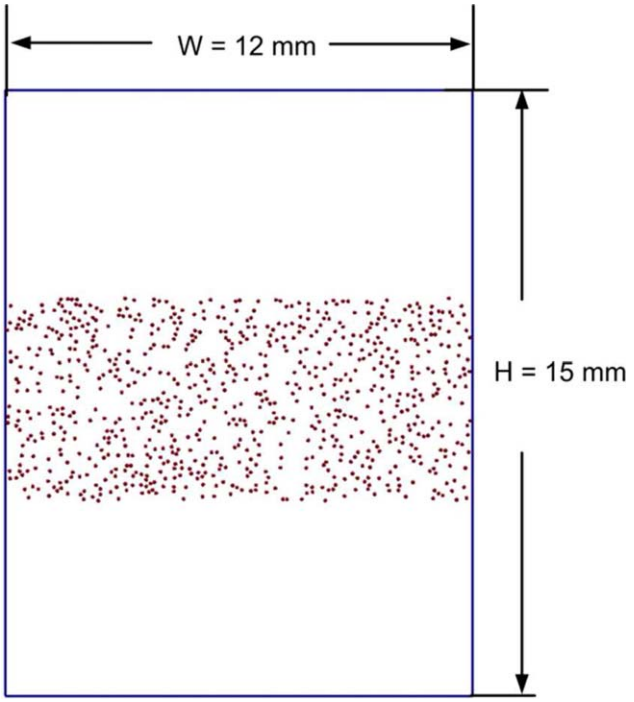

Figure 2. DEM model for deposition of monocharged particles.

[Color figure can be viewed in the online issue, which is available at wileyonlinelibrary.com.]

$$\mathbf{F}_{iM} = \frac{q_i Q_M}{4\pi\varepsilon_0 R_{iM}^2}\mathbf{u}_{iM} \tag{4}$$

where R_{iM} is the distance between the particle center and the center of the cell M; $\mathbf{u}_{iM}$ is the unit vector from cell M to particle i. Equation 4 is used to calculate the electrostatic force between particle i and particles in the cells located in the WI region. In this way, the electrostatic interactions between all particles are considered and the total electrostatic force acting on particle i is then determined by

$$\mathbf{F}_i^{\mathrm{e}} = \sum_{j=1}^{n_{\mathrm{s}}} \mathbf{F}_{ij} + \sum_{M=1}^{N_M} \mathbf{F}_{iM} \tag{5}$$

where n_{s} is the number of neighboring particles in the SI region and N_M is the number of cells in the WI region.

As a cutoff distance, R_{c}, is introduced in both the DT and HPC models, the accuracy of these methods may depend on its value such that the accuracy of the electrostatic forces between particles may increase with increasing values of R_{c}. However, the computational cost will also be increased. To explore the sensitivity of R_{c} values on the performance of these two methods, deposition of monocharged particles in a container in air, similar to those presented by Yu et al.,[25] is modeled using the developed DEM-CFD with various R_{c} values. More details of the deposition of neutral particles which are sensitive to air in a container can be used for reference as reported by Yu et al.[25]

DEM-CFD Model for Deposition of Monocharged Particles

In this study, a two-dimensional (2-D) DEM-CFD model is constructed to simulate the deposition of monocharged particles in a container of a size 12 × 15 mm in air, as shown in Figure 2. Initially, 800 monocharged particles are randomly generated in central horizontal section of the container. The gravitational force and the electrostatic interactions are applied throughout the deposition. When the simulation is initiated, particles start to pack under the gravity and electrostatic forces. The charge on each particle was fixed and the charge transfer was not considered. The material parameters of the particles and the container are given in Table 1. In this study, the charge of the particles is fixed at 2.6×10^{-13} C, which is in the range for pharmaceutical excipient particles with the size of a few hundred microns, such as lactose.[26] Generally, Rayleigh damping,[27] which involves global damping and contact damping, are used in DEM simulations. In this analysis, only contact damping is considered. The damping ratio for particle–particle interactions was set to 0.016, and the damping ratio for particle-wall interactions was set to 0.032, which gives values of the restitution coefficient in the range of 0.90–0.95.[28]

The flow of air is modeled using the CFD scheme. The entire domain is divided into fluid cells with a size of 8 particle radii. The air has a temperature of 293 K and a shear viscosity of 1.8×10^{-5} kg m^{-1} s^{-1}. The initial air pressure is set to the atmospheric pressure of 101,325 Pa. The average molar mass of the air is 2.88×10^{-2} kg mol^{-1}. No-slip boundary conditions are assumed for the flow of the air adjacent to side and bottom surfaces of the container. The upper boundary is set as free outflow. The flow of air is only initiated by the deposition of the particles due to the interaction between the air and the particles.

Both the DT and HPC methods implemented in the DEM-CFD code are used to compute the electrostatic interactions. The cutoff distance, R_{c}, is set to 5d, 15d, and 25d, where d is the particle diameter, for both DT and HPC methods, to examine their sensitivity to this parameter. For the HPC method, the entire domain is divided into cells with a size of 4d to calculate the electrostatic interactions in the WI region. A sensitivity study shows that the cell size in the range of 2–16 particle diameters can provide consistent results (see Discussions section). The evolution of the GT during deposition and the bed height and also the steady-state RDF of the granular bed are analyzed and reported in the next section.

Results

Deposition behavior of monocharged particles

Figure 3 shows the particle profiles at various time instants during the deposition process of neutral particles. It can be seen that the particles keep falling smoothly (Figures 3a, b) until the particles collide with the bottom surface (Figure 3c). Due to the damping effect, the particles eventually settle down at the bottom of the container. A typical close-packed crystalline structure is also observed in the granular bed (Figure 3d).

Table 1. Material Properties of Particles and Container Walls

	Particle	Container
Diameter, d (μm)	100	–
Elastic module, E (GPa)	8.9	210
Poisson ratio, v	0.3	0.3
Density, ρ (kg m^{-3})	1500	7800
Charge, q (C)	2.6×10^{-13}	–

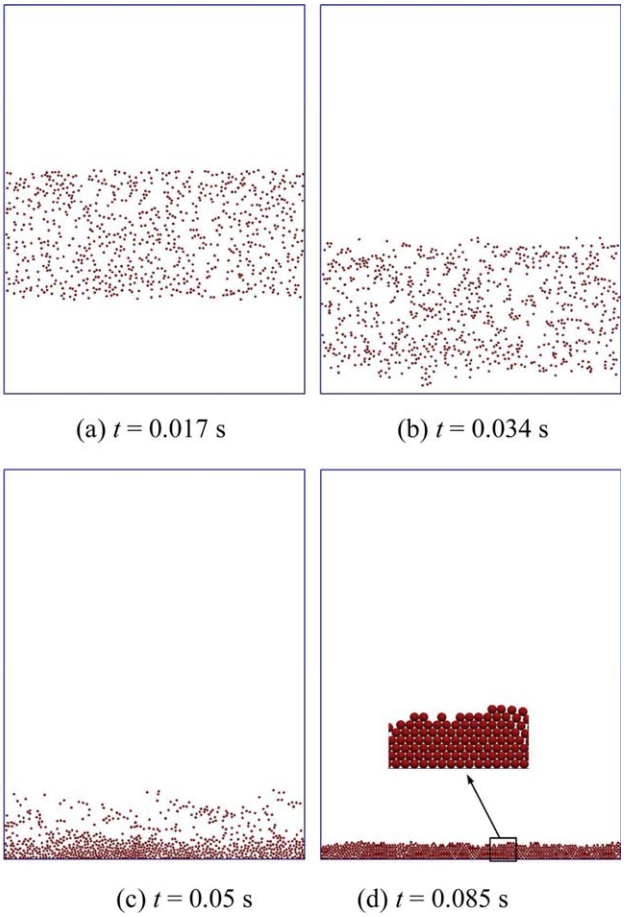

Figure 3. The deposition profiles of neutral particles.

[Color figure can be viewed in the online issue, which is available at wileyonlinelibrary.com.]

Figure 4 shows the particle profiles at various time instants during deposition obtained using the HPC method with $R_c = 15d$. At the beginning of the deposition, as shown in Figure 4a, the charged particles repel each other and move toward the container walls due to the strong repulsive electrostatic forces between the monocharged particles. At the same time, the gravity force causes particles to pack toward the bottom of the container (Figure 4b). Consequently, there is a strong particle oscillation in the granular bed as the gravitational force and the repulsive electrostatic force tend to balance each other. As the initial kinetic energy is gradually dissipated through the contact damping and the friction between the particles and wall, particles start to oscillate around their own equilibrium positions and the kinetic energy of the system fluctuates around a constant value. A dispersed structure of the granular bed, in which the position of the particle is relatively stabilized as shown in Figures 4c, d, is eventually obtained. In addition, it can be seen that a denser structure is obtained at the bottom of the bed compared to that at the top of the granular bed. In other words, the particle concentration gradually decreases from the bottom to the top of the granular bed. It is worth mentioning that, if the attractive image force between the particle and the wall is considered, more particles can be attracted on the walls, depending on material properties and the value of charge.[11] Clearly, the structure of the granular bed of charged particles is different from that of neutral particles. This is attributed to the fact that the particles in the lower region of the particle bed need to stay closer with a smaller interparticle distance that leads to a larger electrostatic repulsive force to support the resultant electrostatic forces from the particles in the upper region.

Wu et al.[6] investigated the self-assembly phenomenon of similarly charged granular particles. In their experiments, a layer of stainless-steel particles were precharged by contact electrification with the base of the polystyrene box, and the box was then tilted by an angle of 9° (Figure 5a). It was found that the gravitational forces acting on the particles were balanced by the repulsive Coulomb force and the particles formed a dispersed structure. The numerical results agree with the experimental observations of Wu et al.,[6] as shown in Figure 5b, in mainly two aspects. First, the particle suspension and dispersion are observed due to the electrostatic repulsive force between similarly charged particles. Second, the particle concentration decrease from the bottom to the top, which is similar to the simulation results. However, it can be seen that there are also some difference between the experimental and numerical results. In the experiment, more layers of particles are concentrated at the bottom. Also, particles at the top are positioned in the central region rather than pushed onto the side walls as shown in Figures 4c and 4d. This is mainly because the charge of the steel sphere in the experiments is relatively small. For instance, the charge-to-mass ratio of the sphere in the experiments is around 9.0×10^{-6} C kg^{-1} which is much smaller than the value of 3.3×10^{-4} C kg^{-1} used in the numerical

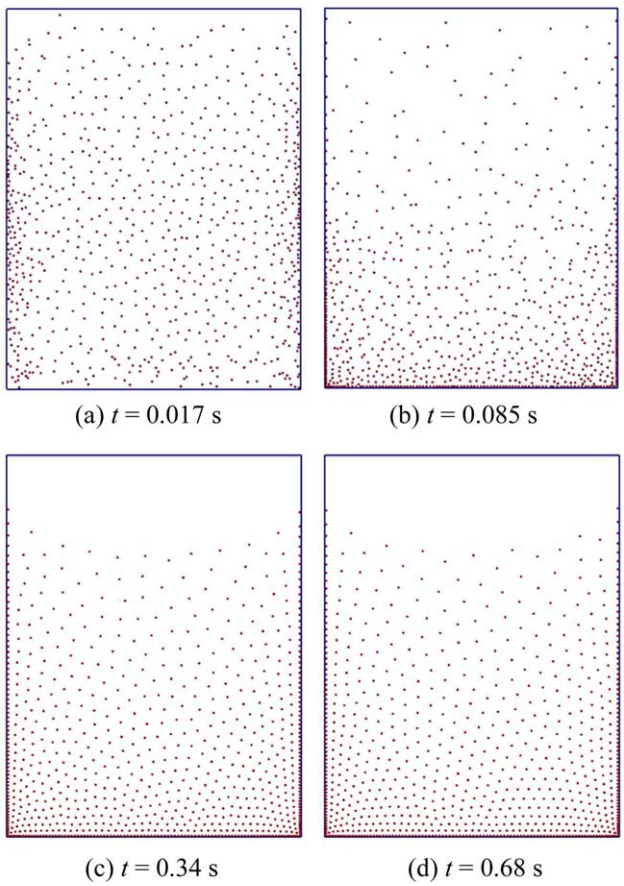

Figure 4. Particle profiles at various time instants obtained with the HPC method ($R_c = 15d$).

[Color figure can be viewed in the online issue, which is available at wileyonlinelibrary.com.]

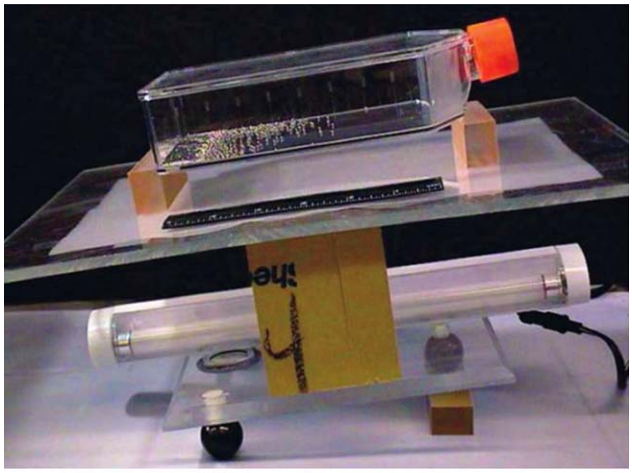

(a) Experimental setup

(b) Particle profile

Figure 5. Packing profile of charged particles obtained experimentally by Wu et al.[6]

Reprinted (adapted) with permission from Wu et al., Ind Eng Chem Res., 2008, 47(15), 5005–5015, © American Chemical Society. [Color figure can be viewed in the online issue, which is available at wileyonlinelibrary.com.]

study. At the same time, the friction between the charged sphere and the polystyrene surface can balance the repulsive force and prohibit particles from moving toward the side walls, especially when the separation distance between particles at the top of the granular bed is relatively large. In the 2-D numerical model, the front and back surfaces do not exist and the friction between the particle and the front and back surfaces is not considered. In addition, the polarization (image effect) between particles and between the particle and the polystyrene surface could also weaken the repulsive force between particles, which have not been considered in the numerical study.

Figure 6 shows the equilibrium states of the granular bed obtained using the DT method with various cutoff distances R_c. It is noticed that the height of the granular bed varies with the cutoff distance; the height of the granular bed increases as the cutoff distance increases. The corresponding packing patterns obtained using the HPC method are shown in Figure 7. In contrary to those observed in Figure 6, a consistent packing pattern is obtained with various cutoff distances. In other words, the packing structure obtained using the HPC method is independent of the cutoff distance specified while the results obtained using the DT method are very sensitive to the specified cutoff distance. The numerical cutoff distance does not exist in reality. This deposition process should be physically deterministic and independent of the numerical cutoff distance. Due to the dependence and sensitivity to the cutoff distance, the DT method can produce artificial errors (Figure 6).

Radial distribution function

The RDF, $g(r)$, is introduced to statistically analyze the packing patterns shown in Figures 6 and 7. The RDF defines the variation of the number density of particles with the distance from a reference particle—a selected individual particle in the particle system, and can effectively describe the radial scattering pattern of a particle system.[29] The RDF of a 2-D inhomogeneous system is defined as

$$g(r)=\frac{n(r)}{2\pi r\sigma\Delta r} \tag{6}$$

where r is the distance from the reference particle; $n(r)$ is the mean number of particles within the ring of width Δr at the distance of r; σ is the mean number density of particles of the entire granular bed. It can be seen that the RDF gives the normalized number density of particles within the region between r and $r+\Delta r$ from the reference particle. In this

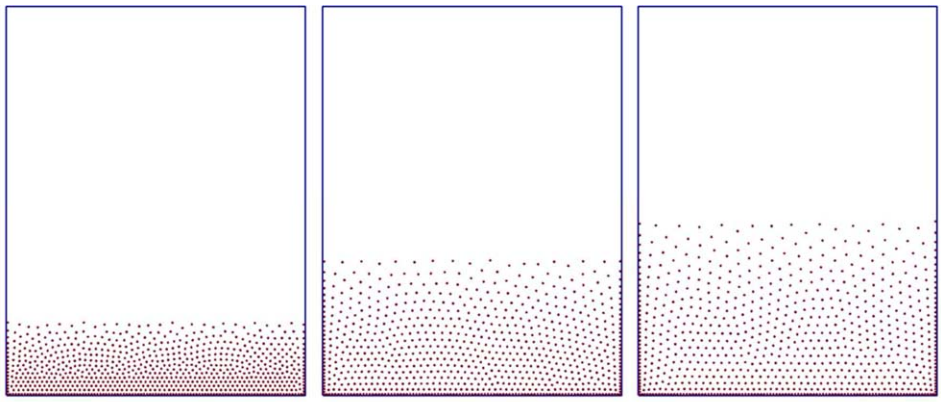

(a) $R_c = 5d$ (b) $R_c = 15d$ (c) $R_c = 25d$

Figure 6. Equilibrium packing patterns obtained using the DT method with different R_c.

[Color figure can be viewed in the online issue, which is available at wileyonlinelibrary.com.]

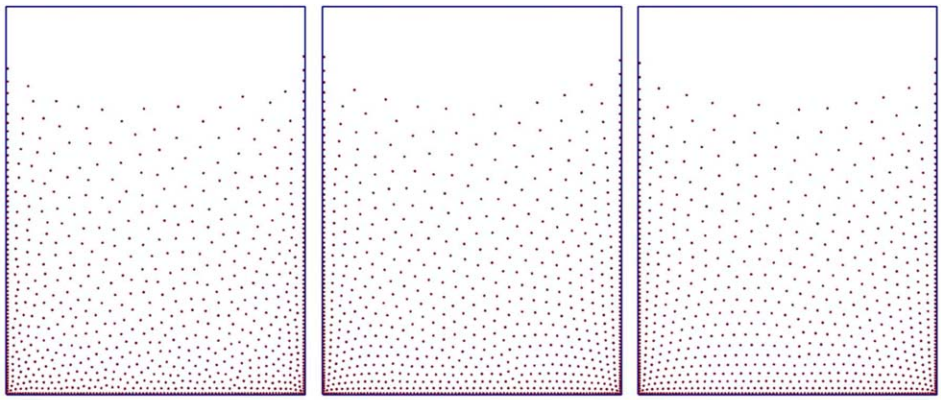

Figure 7. Equilibrium packing patterns obtained using the HPC method with different R_c.

[Color figure can be viewed in the online issue, which is available at wileyonlinelibrary.com.]

study, the average value of RDF for all particles in the system is examined. The value of RDF is sensitive to the value of Δr, especially for the first peak.[29] If Δr is too small, the value of RDF can be extremely large and noisy while if Δr is too large, the RDF profile may miss some major features (peaks) due to the average counting and calculation. In this study, the RDF is determined with r varying from d to $30d$ with an interval of $0.1d$ and Δr is set to $0.1d$, which is similar to the values used by Wu et al.[29]

Figures 8 and 9 show the RDFs for $R_c = 5d$ and $25d$ using the DT and HPC methods. The RDF of neutral particles is also superimposed for reference, which shows a typical hexagonal close-packed pattern with peaks at various separation distances. However, the DT method results in two high peaks that correspond to $R_c = 5d$ and $25d$, which indicates that an artificial dense layer is developed at the specified cutoff distance. However, the RDF profiles obtained using the HPC method are essentially identical when different cutoff distances are specified, which is much more realistic. The data for $R_c = 15d$ follow similar pattern for DT and HPC methods, respectively, and are consequently not shown.

Granular temperature

The GT describes the internal thermal energy of a chaotic particle system. It reflects the fluctuation of particle kinetic energy over the whole system. For a particle system, the GT is defined as[30]

$$T_g = \frac{1}{D}\langle \mathbf{v} - \langle \mathbf{v} \rangle \rangle^2 \tag{7}$$

where the angle bracket $<>$ indicates ensemble averaging; $\mathbf{v}$ is the velocity of each particle; and D is the dimension of the model, which is 2 in this study.

Figure 10 shows the evolution of GTs obtained using the DT method with different values of R_c. The GT of neutral particles is also imposed for reference. During deposition, a peak at about 0.05 s is observed due to the impact between particles and the bottom wall and the change of the velocity (Figure 3c). For charged particles, the GT increases initially as the particles are released to move under gravitational and electrostatic forces. It reaches a maximum value and then starts to decrease, indicating that the system is "cooling down" as the kinetic energy starts to be dissipated through

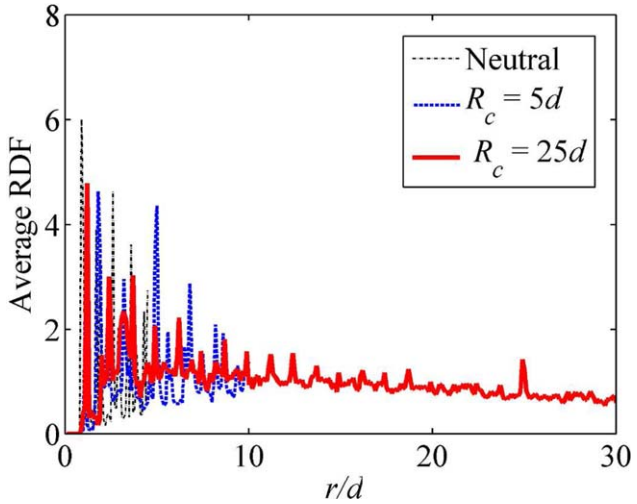

Figure 8. RDF profiles of neutral particles and charged particles obtained using the DT method with different R_c.

[Color figure can be viewed in the online issue, which is available at wileyonlinelibrary.com.]

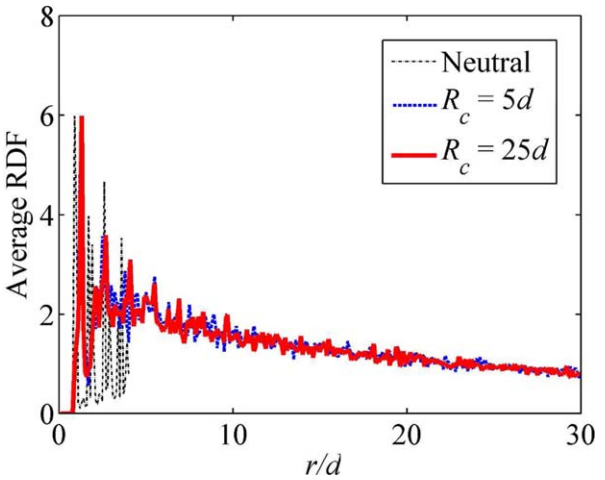

Figure 9. RDF profiles of neutral particles and charged particles obtained using the HPC method with different R_c.

[Color figure can be viewed in the online issue, which is available at wileyonlinelibrary.com.]

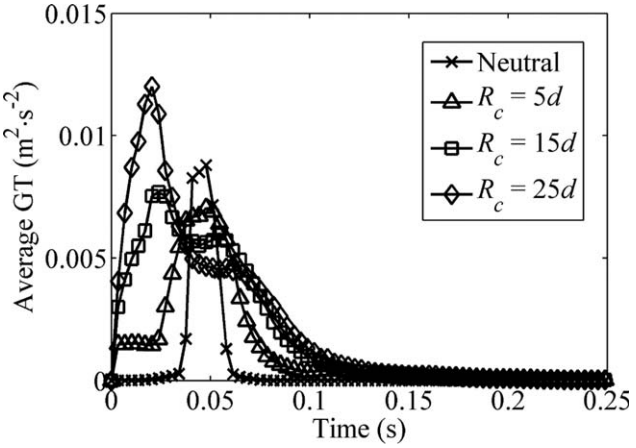

Figure 10. The evolutions of GTs obtained using the DT method for different values of R_c.

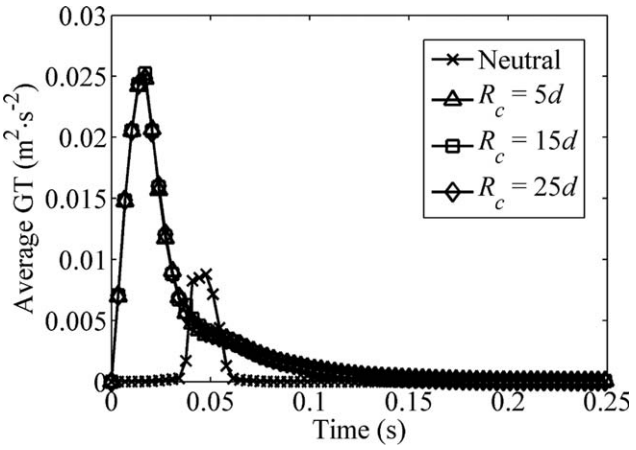

Figure 11. The evolutions of GTs obtained using the HPC method for different values of R_c.

the contacts between particles and walls and the interaction between particles and the air. However, the maximum value increases with increasing R_c with a corresponding reduction in the rate of cooling. In addition, for the shortest cutoff distance (i.e., $R_c = 5d$), there is a dwell period during the heating stage, at which the GT remains unchanged. The corresponding GT data obtained using the HPC method are presented in Figure 11 and they are independent of the value of R_c, which should be the case. In addition, compared to the GTs obtained using the DT method (Figure 10), the maximum value is about a factor two greater.

Discussion

The sensitivity of HPC method to the cell size

The sensitivity of the HPC method to the cell size, d_c, needs to be examined, as the charge of each cell is only the total charge of particles in the cell. A range of cell size ($2d$, $4d$, $8d$, and $16d$) is used in the same model setup as shown in Figure 2 to explore the sensitivity.

Figures 12, 13, and 14 present the packing structure, average RDF, and average GT of monocharged particles using the HPC method with various cell sizes, respectively. The cutoff distance used is $15d$. It can be seen that all the results are of great similarity for various cell sizes. Esselink[8] suggests that for monocharged particles, the sum of the charge of particles in the cell at the center can give a zeroth and up to first-order approximation (if the particles distributes uniformly) for Taylor's expansion. Hoffman[17] further suggests that when collisions between particles occur in the system, a relative larger cutoff distance and smaller cell size can lead to sufficiently accurate Coulomb and collision calculations. In addition, the results can be further improved by considering the center of charge based on the particle positions in the cell instead of the center of the cell.

DT and HPC methods

Figures 6–11 show that, even for the same deposition process with monocharged particles, using the DT method, the height of the granular bed increases with increasing cutoff distance, there is a strong correlation between the peak in the RDF and the cutoff distance, and the evolution of the GT is very sensitive to the specified cutoff distance. These observations are physically unrealistic, as the cutoff distance is only a simulation parameter that should not have such a significant impact on the microstructure of the deposited particle system and thermal behavior during the deposition process. These unrealistic results were obtained because the repulsive electrostatic forces between particles with a separation distance longer than the cutoff distance are completely ignored in the DT method. As a consequence, particles experience weaker electrostatic forces with a smaller cutoff distance. To counterbalance the gravity of the particles, smaller interparticle distances and larger electrostatic forces are necessary. Therefore, a more compact packing structure is induced as observed in Figure 6.

In 2-D simulations using the DT method, the circle at the cutoff distance of each particle acts as a critical and equilibrium boundary for the combined effects of gravitational and electrostatic repulsive forces. Particles under gravity tend to deposit onto the bottom of the container and pack together while the electrostatic repulsive force between monocharged particles will dilate the particle system. For each pair of particles, when the electrostatic force is larger than the gravitational force, particles move away from each other until the distance between particles reaches the cutoff distance. As the particles move further away from each other (i.e., beyond the cutoff distance), the electrostatic force between particles is ignored and the particles start to pack together because of the gravitational force. Once the distance between the particles is smaller than the cutoff distance, the electrostatic force is activated again. So, each pair of particles vibrates about the cutoff distance and eventually achieve the equilibrium state due to the contact damping and friction between the particles and walls. Therefore, a strong peak at the cutoff distance is induced in the RDF profile. However, when the cutoff distance is larger, the electrostatic force at the corresponding cutoff distance becomes weaker and the corresponding value of RDF is much smaller. This artificial effect has also been observed in MD and Monte Carlo simulations,[31–33] showing that artificial layers located at the cutoff distances were observed when the truncation method was used to describe the thermodynamics of aqueous ionic solutions.

It has been shown that the GT obtained using the DT method is much lower than that using the HPC method due to the neglect of the electrostatic potential from the long-range region. As only the electrostatic forces within the

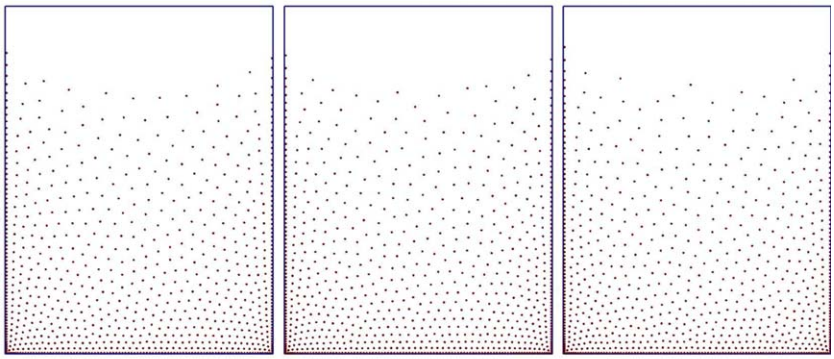

(a) $d_c = 2d$ (b) $d_c = 8d$ (c) $d_c = 16d$

Figure 12. The packing structure of monocharged particles using HPC method with various cell sizes.

[Color figure can be viewed in the online issue, which is available at wileyonlinelibrary.com.]

cutoff distance are considered in the DT method, the particles in the simulations with smaller cutoff distances experience a smaller electrostatic repulsive force at the initial stage and possess smaller electrostatic energy, which leads to a smaller acceleration and a smaller velocity difference (i.e., GT). Initially, particles are accelerated to move away from each other because of the electrostatic repulsion and this results in an increase of GT. As the distance between particles becomes larger than the cutoff distance, the electrostatic force and the subsequent acceleration are ignored in the simulation and consequently the GT remains unchanged. When the particles reach the bottom of the container and consolidate under gravity, the distance between particles becomes smaller than the cutoff distance again. The GT starts to increase and eventually achieves the maximum value. Moreover, when the cutoff distance is larger, the ignored electrostatic interaction becomes less significant, and its influence on the GT of particle system is also smaller.

In the HPC method, all potential electrostatic interactions are considered. Even though an approximation is made to calculate the electrostatic forces in the WI region (i.e., with a separation distance larger than the cutoff distance) using the cumulative net charge in a cell (Eqs. 3–5) instead of a direct calculation of particle–particle interactions, the results illustrated that this approximation is appropriate and produces more consistent results than the DT method. In particular, it is demonstrated that the HPC method is insensitive to the cutoff distance specified (Figures 7, 9, and 11).

The computational time and accuracy of DT and HPC methods

Position B (PB). A series of DT simulations with larger cutoff distance ($50d-125d$) is performed to further confirm the computational efficiency and accuracy. The packing structure, RDF, and GT are shown in Figures 15, 16, and 17, respectively. It can be seen that for the DT method, when the cutoff distance is larger than $100d$ in the chosen values, the packing structure, RDF, and GT start to show similar patterns to those obtained from the HPC method, as expected. This is because when the cutoff distance is large enough (e.g., larger than the dimension of the granular bed), all (or almost all) electrostatic repulsive forces between particles are considered, so that the DT method produces more accurate results similar to the HPC method. Conversely, the results indicates that the HPC method produces sufficiently accurate results compared to those computed from all repulsive forces between particles. As shown in Figure 18, the computational time of the DT method with larger cutoff distances (e.g., $>100d$) is greater than that of the HPC method

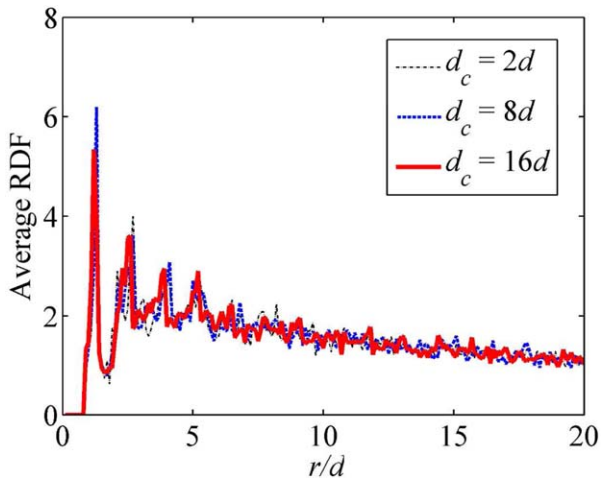

Figure 13. The average RDF of monocharged particles using HPC method with various cell sizes.

[Color figure can be viewed in the online issue, which is available at wileyonlinelibrary.com.]

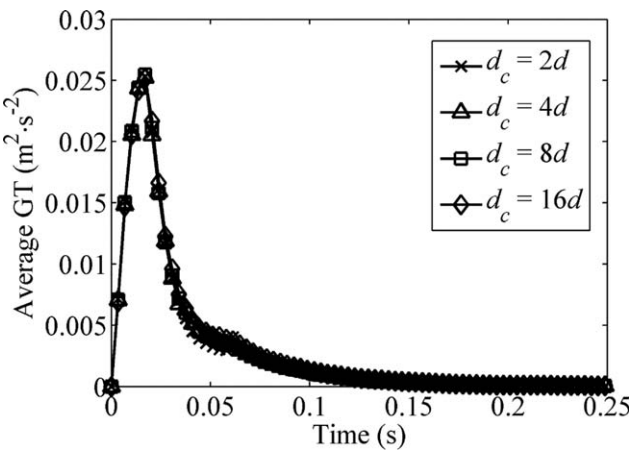

Figure 14. The average GT of monocharged particles using HPC method with various cell sizes.

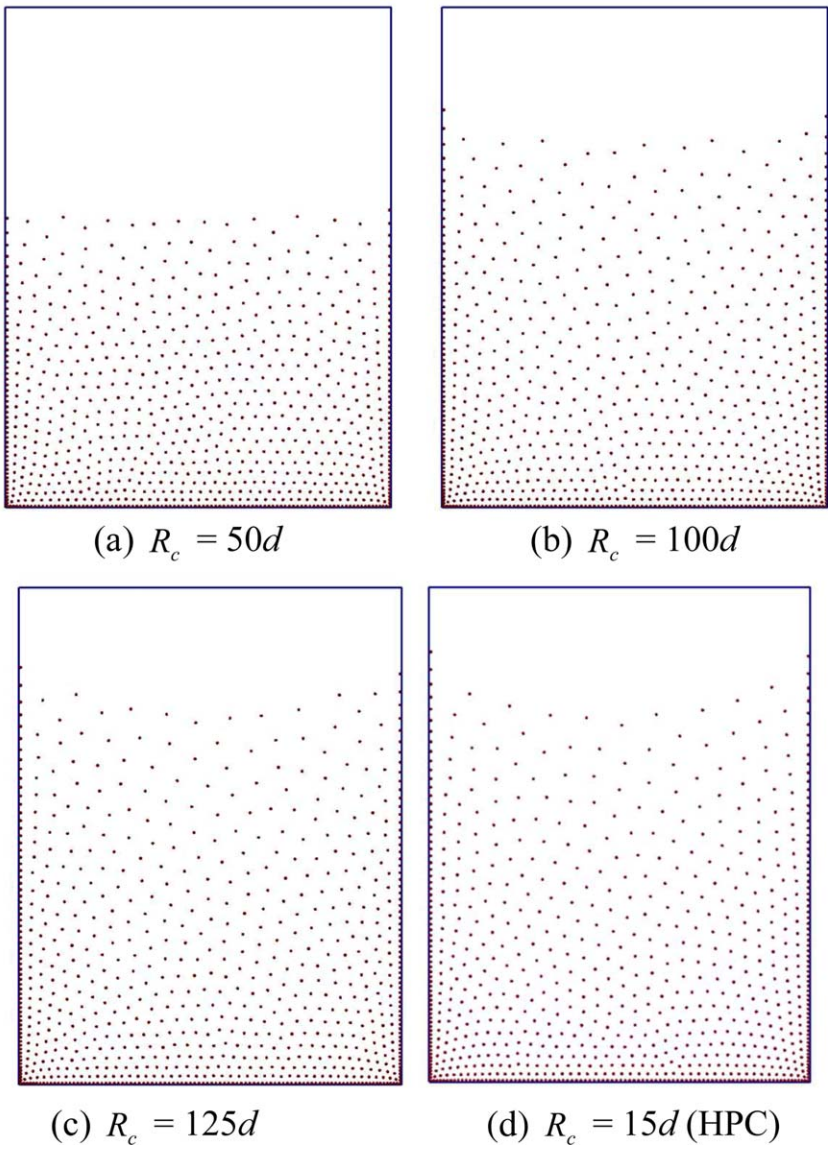

Figure 15. The packing structure from DT simulations with larger cutoff distance (50*d*−125*d*).

[Color figure can be viewed in the online issue, which is available at wileyonlinelibrary.com.]

with the same results (e.g., 15*d*). In this study, only 800 particles are considered, so the difference of the computational times between the HPC method and the DT method with a sufficiently large cutoff distance (e.g., $>100d$) is not very significant. If a large number (e.g., millions) of particles are involved, the DT method with a sufficiently large cutoff distance can take a significant amount of computational time or even became impossible to use.

The cutoff distance can also affect the computational time for the DT and HPC methods. To compare the difference between these two methods, the computational time for simulations with different cutoff distances were obtained (with Intel Xeon CPU E5–2650 0 @ 2.00 GHz) at the same physical time of 0.68 s as shown in Figure 18. It is can be seen that the DT method is more sensitive to the cutoff distance than the HPC method. For the DT method, it takes 15.9–34.0 h when the cutoff distance varies from 5*d* to 25*d*. The computational time is increased by more than two times. The HPC simulations takes more hours and the computational time is also weakly dependent on the cutoff distance. This is due to the consideration of electrostatic interaction in both the SI and WI regions. In these two regions, similar computations are implemented to calculate the electrostatic interactions for each reference particles. Although the change of cutoff distance from 5*d* to 25*d* can alter the sizes of the two regions, it will not significantly affect their total computation cost. It should also be noted that for the HPC method, the computational time increases with the increase of the cutoff distance, especially when a relatively large cut-off distance is chosen (e.g., 125*d*) and more particle–particle interactions are considered (Figure 18).

Although the results produced by the HPC method are insensitive to the cutoff distance, its accuracy is still limited. The electrostatic force is a function of the charge of objects and the distance between them. However, from Figure 1 and Eq. 3, it can be seen that the charge of a cell is a simple summation of the charge of the particles without considering the distance between each particle and the center of the cell. Consequently, the electrostatic force between the reference particle and the cell cannot accurately represent the actual

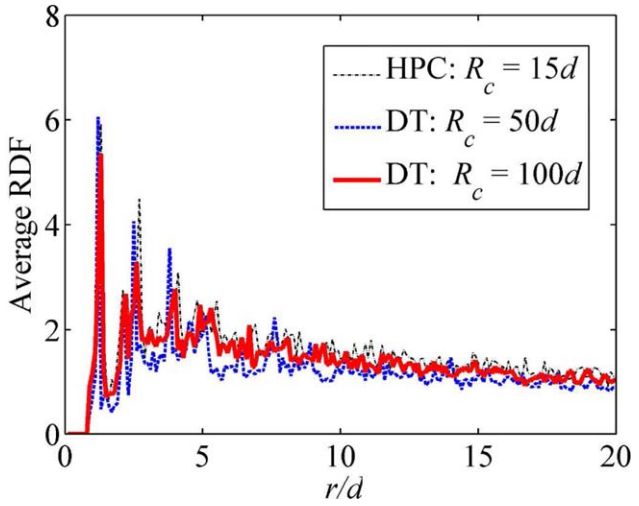

Figure 16. The average RDF from DT simulations with larger cutoff distance (50*d*−125*d*).

[Color figure can be viewed in the online issue, which is available at wileyonlinelibrary.com.]

force between the reference particle and those in the cell. To obtain a high order of accuracy, a multipole expansion method[8,16,17] can be used to approximate the charge of the particles onto the center of the corresponding cell. Moreover, the image and polarization effects that affect the electrostatic interactions between closely positioned particles should also be considered in the future.

In this study, only monocharged particles are used for investigation. When bicharged particles are involved in the particle system, the agglomerates and aggregates can be formed due to the mutual attraction and repulsion. Due to the long-range nature, it takes more energy to break the agglomerates induced by long-range electrostatic interactions than the short-range interaction (e.g., JKR model for surface molecular attractions during contact) with the same maximum magnitude.[34] Although the electric field induced by oppositely charged particles (dipole) decreases more rapidly with the distance, as r^{-3},[16] further studies on polycharged and oppositely charged particles should be considered in detail as well. In addition, although the HPC method is used to model the flow of particles with fixed charge in air, it can also be extended to investigate the flow and transfer of

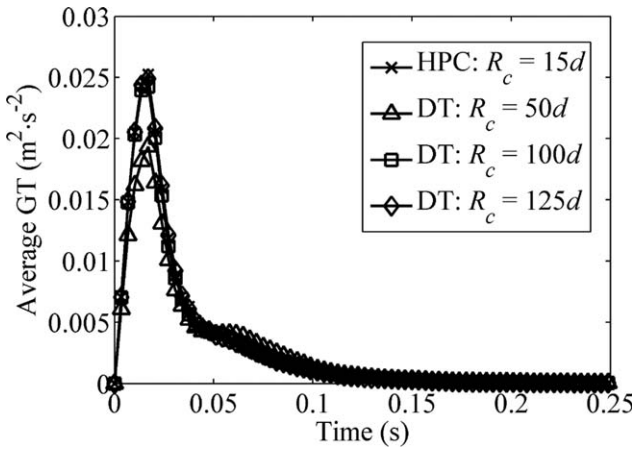

Figure 17. The average GT from DT simulations with larger cutoff distance (50*d*−125*d*).

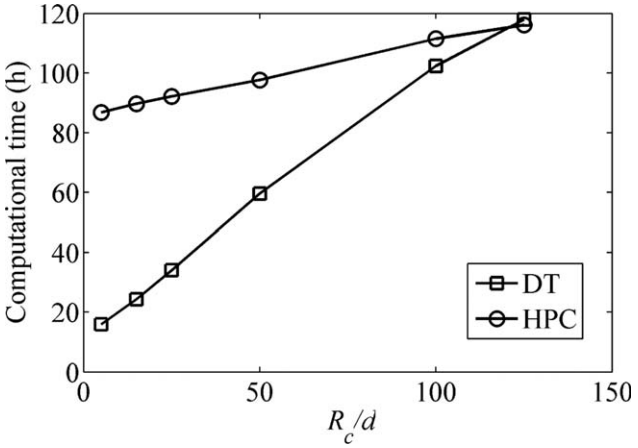

Figure 18. The computation time of DT and HPC methods for a simulation of physical time of 0.68 s.

charges (electrons) in different media, such as conductive and semiconductive materials and packed granular beds.[35]

Conclusions

To model charged particle systems with DEM-CFD, long-range electrostatic interactions should be considered and carefully implemented. In this study, a simple DT method and a HPC method, both using a cutoff distance to improve the computation efficiency, are implemented into an in-house DEM-CFD code, which is then used to model the deposition of monocharged particles. The sensitivity of both methods to the cutoff distance is examined. It was found that the DT method is very sensitive to the cutoff distance and the neglect of the weak electrostatic interactions between particles with a separation distance larger than the cutoff distance introduces significant errors. This implies that the weak electrostatic interactions should not be completely ignored in DEM-based modeling, especially for monocharge particle systems. As an alternative, these WIs are approximated using the particle-cell approach in the HPC method. It has been shown that this method is not sensitive to the cutoff distance, and more accurate and consistent results are obtained for the deposition of monocharged particle systems, compared to the DT method. It is hence demonstrated that the HPC method will offer a robust and accurate approach for modeling the long-range electrostatic interactions in DEM.

Acknowledgment

This project is fully funded by Sanofi (previously Sanofi-Aventis).

Literature Cited

1. Matsusaka S, Maruyama H, Matsuyama T, Ghadiri M. Triboelectric charging of powders: a review. *Chem Eng Sci*. 2010;65(22):5781–5807.
2. Pei C, Wu C-Y, England D, Byard S, Berchtold H, Adams M. Numerical analysis of contact electrification using DEM–CFD. *Powder Technol*. 2013;248:34–43.
3. Pei C, Wu C-Y, Adams M, England D, Byard S, Berchtold H. Contact electrification and charge distribution on elongated particles in a vibrating container. *Chem Eng Sci*. 2014;125:238–247.

4. Grzybowski BA, Winkleman A, Wiles JA, Brumer Y, Whitesides GM. Electrostatic self-assembly of macroscopic crystals using contact electrification. *Nat Mater*. 2003;2(4):241–245.
5. Pei C, Wu C-Y, Byard S, England D. Numerical analysis of electrostatic effects during powder deposition using DEM/CFD. *J Pharm Pharmacol*. 2010;62(10, SI):1454–1455.
6. Wu SC, Wasan DT, Nikolov AD. Two-dimensional self-assembly of similarly charged granular particles. *Ind Eng Chem Res*. 2008; 47(15):5005–5015.
7. Kolikov K, Ivanov D, Krastev G, Epitropov Y, Bozhkov S. Electrostatic interaction between two conducting spheres. *J Electrostat*. 2012;70(1):91–96.
8. Esselink K. A comparison of algorithms for long-range interactions. *Comput Phys Commun*. 1995;87(3):375–395.
9. Bichoutskaia E, Boatwright AL, Khachatourian A, Stace AJ. Electrostatic analysis of the interactions between charged particles of dielectric materials. *J Chem Phys*. 2010;133(2):024105.
10. Bailey AG. Electrostatic phenomena during powder handling. *Powder Technol*. 1984;37(1):71–85.
11. Korevaar MW, Padding JT, Van der Hoef MA, Kuipers JAM. Integrated DEM–CFD modeling of the contact charging of pneumatically conveyed powders. *Powder Technol*. 2014;258:144–156.
12. Hockney RW, Eastwood JW. *Computer Simulation Using Particles*. Bristol, New York: Adam Hilger, 1988.
13. Dawson JM. Particle simulation of plasmas. *Rev Mod Phys*. 1983; 55(2):403–447.
14. Luty BA, VanGunsteren WF. Calculating electrostatic interactions using the particle-particle particle-mesh method with nonperiodic long-range interactions. *J Phys Chem*. 1996;100(7):2581–2587.
15. Shimada J, Kaneko H, Takada T. Efficient calculations of coulombic interactions in biomolecular simulations with periodic boundary-conditions. *J Comput Chem*. 1993;14(7):867–878.
16. Liu G, Marshall JS, Li SQ, Yao Q. Discrete-element method for particle capture by a body in an electrostatic field. *Int J Numer Methods Eng*. 2010;84(13):1589–1612.
17. Hoffmann R. DEM simulations of toner particles with an O (N log N) hierarchical tree code algorithm. *Granul Matter*. 2006;8(3–4):151–157.
18. Kafui KD, Thornton C, Adams MJ. Discrete particle-continuum fluid modelling of gas-solid fluidised beds. *Chem Eng Sci*. 2002;57(13): 2395–2410.
19. Guo Y, Kafui KD, Wu CY, Thornton C, Seville JPK. A coupled DEM/CFD analysis of the effect of air on powder flow during die filling. *AIChE J*. 2009;55(1):49–62.
20. Guo Y, Wu C, Thornton C. Modeling gas-particle two-phase flows with complex and moving boundaries using DEM-CFD with an immersed boundary method. *AIChE J*. 2013;59(4):1075–1087.
21. Zhu HP, Zhou ZY, Yang RY, Yu AB. Discrete particle simulation of particulate systems: theoretical developments. *Chem Eng Sci*. 2007;62(13):3378–3396.
22. Hogue MD, Calle CI, Weitzman PS, Curry DR. Calculating the trajectories of triboelectrically charged particles using discrete element modeling (DEM). *J Electrostat*. 2008;66(1–2):32–38.
23. Johnson KL. *Contact Mechanics*. Cambridge: Cambridge University Press, 1985.
24. Mindlin RD, Deresiewicz H. Elastic spheres in contact under varying oblique forces. *J Appl Mech ASME*. 1953;20(3):327–344.
25. Yu S, Guo Y, Wu C-Y. DEM/CFD modelling of the deposition of dilute granular systems in a vertical container. *Chin Sci Bull*. 2009; 54(23):4318–4326.
26. Watanabe H, Ghadiri M, Matsuyama T, Ding YL, Pitt KG, Maruyama H, Matsusaka S, Masuda H. Triboelectrification of pharmaceutical powders by particle impact. *Int J Pharm*. 2007;334(1–2): 149–155.
27. Mohammad DRA, Khan NU, Ramamurti V. On the role of Rayleigh damping. *J Sound Vib*. 1995;185(2):207–218.
28. Hu G, Hu Z, Jian B, Liu L, Wan H. On the determination of the damping coefficient of non-linear spring-dashpot system to model Hertz contact for simulation by discrete element method. *J Comput*. 2011;6(5):984–988.
29. Wu SC, Wasan DT, Nikolov AD. Structural transitions in two-dimensional hard-sphere systems. *Phys Rev E*. 2005;71:056112.
30. Goldhirsch I. Introduction to granular temperature. *Powder Technol*. 2008;182(2):130–136.
31. Brooks CL, Pettitt BM, Karplus M. Structural and energetic effects of truncating long ranged interactions in ionic and polar fluids. *J Chem Phys*. 1985;83:5897–5908.
32. Brooks CL. The influence of long-range force truncation on the thermodynamics of aqueous ionic-solutions. *J Chem Phys*. 1987;86(9): 5156–5162.
33. Takahashi K, Narumi T, Yasuoka K. Cutoff radius effect of the isotropic periodic sum method in homogeneous system. II. Water. *J Chem Phys*. 2010;133(1):014109.
34. Moreno-Atanasio R, Antony SJ, Williams RA. Influence of interparticle interactions on the kinetics of self-assembly and mechanical strength of nanoparticulate aggregates. *Particuology*. 2009;7(2):106–113.
35. Antony SJ, Stockwell B. Influence of particle-scale properties on the charge transfer characteristics in semiconducting particulate packing: particle-based finite element analysis. *Adv Powder Technol*. 2007; 18(6):795–801.

Manuscript received Oct. 2, 2014, and revision received Jan. 15, 2015.